Effect of radiation on the crystals of polyethylene and paraffins: 3. Irradiation in the electron microscope

G. Ungar*, D. T. Grubb† and A. Keller
HH Wills Physics Laboratory, University of Bristol, Tyndall Avenue, Bristol BS8 1TL, UK

Paraffins were irradiated with electrons in the electron microscope. The electron microscopic image and the electron diffraction patterns were followed as a function of dose. The objectives were: (a) to establish a connection between the 'polyethylene-type' and 'paraffin-like' behaviour identified in Parts 1 and 2, respectively; and (b) to identify the phase segregation, which has emerged in Part 2, by visual means.

(a) Increasing chain length, increasing dose rate (at levels such as realisable only with electrons) and decreasing temperature individually and in combination, were found to favour the 'polyethylene-type' behaviour (crystal destruction through increasing lattice defects) while the reverse trend of the above three variables favoured the 'paraffin-like' behaviour (phase-segregated damaged and undamaged species).

(b) Segregated phases could under some circumstances be identified as non-diffracting 'droplets' within a crystalline matrix, with the lattice hardly affected, in the electron microscopic image. These droplets remain constant in number but increase in size as the irradiation progresses, the number of droplets depending on the chain length of the paraffin, on the irradiation temperature and on the dose rate. This behaviour, together with some further observations, reveals that the radiation-induced active species do not form crosslinks *in situ* but migrate over distances which can amount to μm. In contrast to the above, in the case of the lowest paraffin investigated, ($C_{23}H_{48}$), the lattice became uniformly distorted as judged from the diffraction pattern, but the damage was observed to 'heal-out' with time. Considering this evidence, phase segregation may thus occur in two ways: (i) the crosslinks form in the liquid phase subsequent to the nucleation of such a phase; (ii) the crosslinks are produced originally within the lattice but subsequently become excluded from it. Both cases are examples of the extreme inhomogeneity of the lattice damage (also supported on a molecular level, by an analysis of the crosslinked products by g.p.c.[20,21]) involving migration of the active precursor species and of the actual crosslinked material respectively. All this has implications for the underlying radiation chemistry, for molecular mobility and compatibility of the systems.

INTRODUCTION

The present series of prelimary reports dealing with the effects of radiation on polyethylene (PE) and paraffin crystals[1,2] will be concluded with an account of experiments performed in the electron microscope (*EM*). Studies of a similar kind have already been pursued in the past[3-7]. Radiation damage has continually represented a major obstacle in *EM* investigations of organic materials[8,9]. Irradiation experiments performed in the *EM* offer certain advantages over those using γ-irradiation, in that the crystals can be directly observed, and their diffraction recorded, while they are being irradiated. Furthermore, higher dose rates are used. However, fullest advantage can be taken of the *EM* results if they are considered in conjunction with other evidence, such as the previously reported findings on γ-irradiated crystals[1,2]. Whereas this paper reports only selected experimental material, the complete results will be presented later.

* Present address: Rudjer Bosković Institute, POB 1016, 41001 Zagreb, Yugoslavia.
† Present address: Department of Materials Science, Cornell University, Bard Hall, Ithaca, NY 14853, USA.

0032-3861/80/111284-08$02.00

EXPERIMENTAL

The n-alkanes used in the present experiments and their melting temperatures are listed in *Table* 1. Specimens were prepared by evaporating a drop of dilute solution on carbon film. Solution-grown single crystals of PE were also investigated.

The electron microscope used was a Phillips EM 301, fitted with a heating–cooling stage. The beam current was measured with an electrometer attached to the viewing screen and the collection efficiency of the screen was determined by comparison with a Faraday cup[10]. The current density was varied from 13 to 400 mA m^{-2}, as measured in the sample plane. Considering the voltage

Table 1 n-Alkanes used in the *EM* experiments

n-Alkane	Formula	Melting point (°C
Tricosane	$C_{23}H_{48}$	47
Octacosane	$C_{28}H_{58}$	61
Tetracontane	$C_{40}H_{82}$	80.5
Tetrananocontane	$C_{94}H_{190}$	113.8*

* Data by H. W. Wyckoff, quoted by Broadhurst[23]

used (100 kV) and the crystals investigated, this was equivalent to abosrbed dose rates of between 0.3 and 10 Mrad h^{-1} [9].

RESULTS

Bright field images

Sequences of bright field micrographs of paraffin crystals were recorded in order to observe possible changes in morphology induced by electron irradiation. Crystals were observed both at room and at elevated temperatures. Paraffin $C_{40}H_{82}$ was examined in greatest detail. The observed contrast was primarily due to *hk*O diffraction.

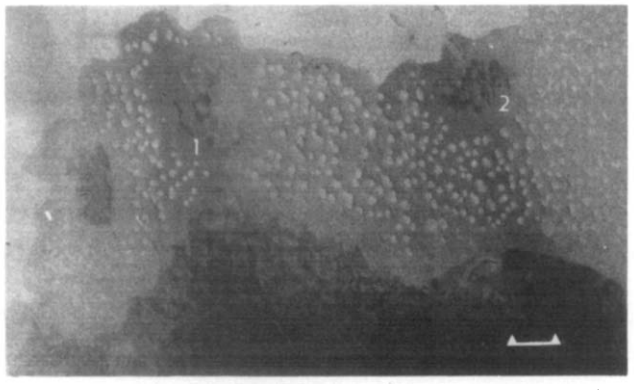

Figure 1 Crystal of $C_{40}H_{82}$ after passing a charge of 16 C m^{-2} at 57°C. Bar = 1 μm

Irradiation of $C_{40}H_{82}$ at room temperature produces no clear heterogeneity. After a crystal is brought into the beam the Moiré patterns disappear first while the bend contours broaden and later vanish as well. The overall image weakens progressively. At a dose of about 100 Coulomb m^{-2} all crystalline diffraction disappears and only a faint image remains. Such behaviour indicates that crystallinity becomes destroyed by increasing distortion of the crystal lattice. Crystals of $C_{94}H_{190}$ behave similarly when irradiated both at room and at higher temperatures, up to about 10°C below the melting point. An increase in temperature accelerates the whole process of crystallinity destruction.

A different situation results when crystals of $C_{40}H_{82}$ are irradiated above room temperature. The main feature in this case is the formation of discrete round-shaped non-diffracting regions within the crystals which, otherwise, remain little affected. An example is shown in *Figure* 1. The largest area in this micrograph is covered by a thin crystal layer, to be referred to as a 'single layer', with darker patches corresponding to overgrowth layers. Two wide, vertically-oriented extinction contours can be seen, and there the contrast between the diffracting cyrstal and the non-diffracting patches is highest. Further away from the bend contours this contrast almost disappears as the crystal tilts away from the diffracting position.

A complete sequence of micrographs, taken at increasing radiation dosages at 57°C, is presented in *Figure* 2. Here we see a smaller area of the $C_{40}H_{82}$ crystal shown in the previous photograph. *Figure* 1 itself was taken at a dose intermediate between those of *Figures* 2*b* and 2*c*. The non-diffracting regions are seen to have appeared already at a low dose, spreading at the expense of the diffracting

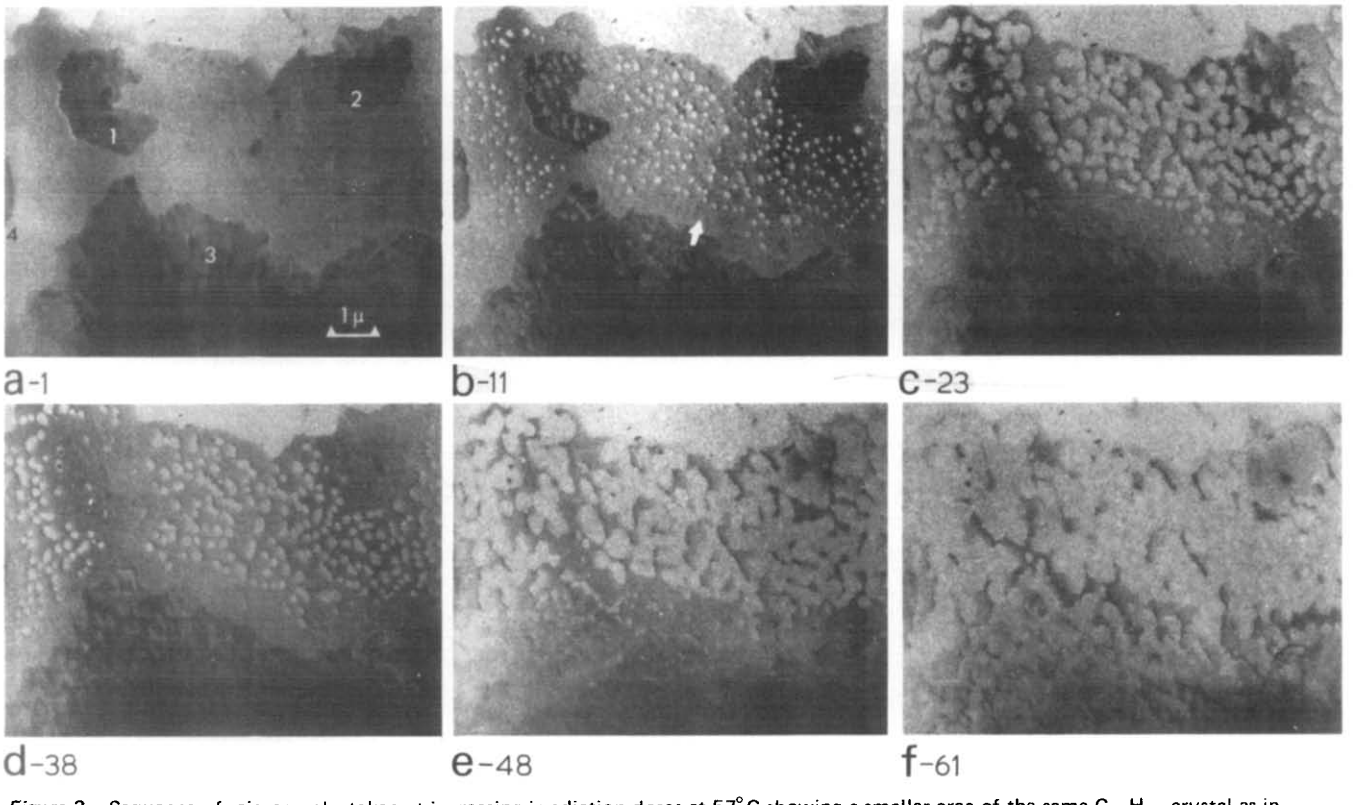

Figure 2 Sequence of micrographs taken at increasing irradiation doses at 57°C showing a smaller area of the same $C_{40}H_{82}$ crystal as in *Figure 1*. Current density 100 mA m^{-2}. Numbers under each micrograph show the dose in C m^{-2}. Exposures were taken at the following times, in minutes, counting from the start of irradiation: (a) 0; (b) 1.5; (c) 3.7; (d) 6; (e) 7.5; and (f) 9.6

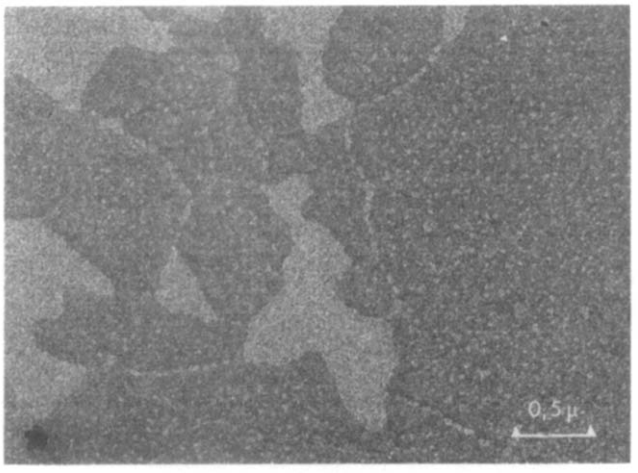

Figure 3 Group of crystals of $C_{40}H_{82}$ after irradiation with 33 C m^{-2} at 40°C; current density 100 mA m^{-2}

crystal as irradiation proceeds. While decreasing in area the remaining crystalline portion is not greatly affected. Thus, for instance, Moiré fringes from superposed crystal layers can still be observed at a dose of 23 Coulomb m^{-2} (not visible in the print). The electron diffraction pattern, although becoming weaker, barely changes otherwise (see below). Changing the electron current, i.e. the dose rate, alters the situation to a certain extent. Decreasing the dose rate results in fewer but larger non-diffracting regions, while increasing it has the opposite effect.

Situations intermediate between those produced at room temperature and 57°C irradiations arise at intermediate temperatures. The non-diffracting regions appear at a later stage. For a given dose they are more numerous and smaller than those produced at 57°C. *Figure* 3 shows a large number of small white specks in a crystal of $C_{40}H_{82}$ irradiated at 40°C. The remaining cyrstalline phase is now more distorted than at 57°C: the diffraction contrast weakens with dose and the bend contours broaden greatly (already absent in *Figure* 3).

The heterogeneities, which in $C_{40}H_{82}$ crystals occur only at elevated temperatures, are observed in crystals of $C_{28}H_{58}$ both at elevated and at room temperature. The behaviour of $C_{28}H_{58}$ at room temperature is similar to that of $C_{40}H_{82}$ at about 50°C.

There are a number of interesting details to be noted in the images of partly destroyed paraffin crystals. Some of them will be dealt with in the Discussion, whereas some will not be discussed here. At this stage we shall draw attention to three points: cyrstal topography, the position of the non-diffracting regions in a multilayered crystal and the nature of the non-diffracting regions.

The importance of establishing the exact topography of the multilayered cyrstal will become apparent in the Discussion. Here, we deduce that the crystal overgrowth faces the carbon film, while the single layer overlies it, as schematically sketched in *Figure* 4. This is concluded from the existence of bright bend contours at the edges of overgrowth layers — see, for example, the thin bright line along the left edge of overgrowth 1 in *Figure* 2*a*. Such a topography seems a natural consequence of the mode of sample preparation: as the drop of solution evaporated, a thin crystalline skin ('single layer') formed first on its surface, while subsequently the overgrowth crystallized at the inner side of the skin. Eventually as the crystal became deposited on the carbon substrate, the situation in *Figure* 4 resulted. The 'single layer' most often contained two molecular layers (≃10 nm thickness), but layers with thicknesses equivalent to one, three or more molecular lengths were also observed. This was revealed by application of a shadowing technique.

The next point to mention is that the non-diffracting regions always appear first in the overgrowth (evidence from micrographs not shown here), and that the crystal overgrowth becomes destroyed more rapidly than the single layer (see *Figure* 2). One of the indications that the non-diffracting patches are indeed located in the overgrowth, and not in the overlying single layer, is their non-uniform contrast, as for instance in overgrowth 1, *Figure* 2*b*. The patches have darker centres compared with the periphery. This is interpreted as resulting from bending (inwards or outwards) of the overlying crystalline single layer above the non-diffracting areas of the overgrowth. If it was the bottom layer (i.e. that lying on the carbon substrate) which had remained undamaged, it would not have become bent, regardless of what happened to the upper layer. There are also other indications, which cannot be itemized here in brief, which leave little doubt that the non-diffracting regions are indeed located in the overgrowth layer.

The problem of the nature of the non-diffracting patches can be reduced to the question of whether the lack of diffraction is due to absence of material or merely to lack of crystallinity. That the material remains at its original location after its diffracting ability has been destroyed is seen, for instance, in *Figure* 2*c* or in *Figure* 1. After the destruction of overgowths 1 and 2 the areas originally covered by them remain slightly darker than the surrounding crystal. This is attributed to the additonal contrast produced by the amorphous layer which remains sandwiched between the carbon film and the still-crystalline single layer.

Implying that the non-diffracting patches were caused by actual removal of irradiated material, for example by evaporation of radiolytic products, would also contradict the known radiation chemistry of n-alkanes. The amount of chain scission is far from sufficient to produce such an effect[11]. The non-diffracting patches will be assumed to be a liquid or a crosslinked gel, since only these can be the states of an amorphous paraffin at room temperature. They will therefore be referred to as 'droplets'.

It should be stressed that the changes described in this paper are a direct consequence of irradiation, and are not due to heating in the electron beam. The increase in temperature of such thin crystals in contact with the conducting carbon substrate cannot exceed more than a fraction of degree when exposed to the currents used here[8,9].

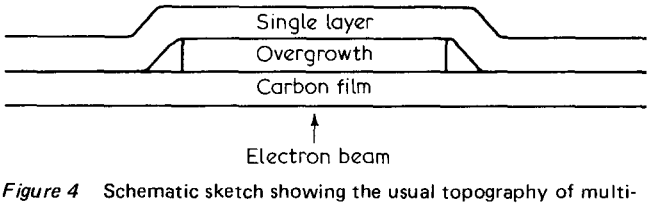

Figure 4 Schematic sketch showing the usual topography of multilayered crystals in the present experiments. The position of the specimen in the *EM* was such that the crystals were facing downward, with the electron beam coming from above

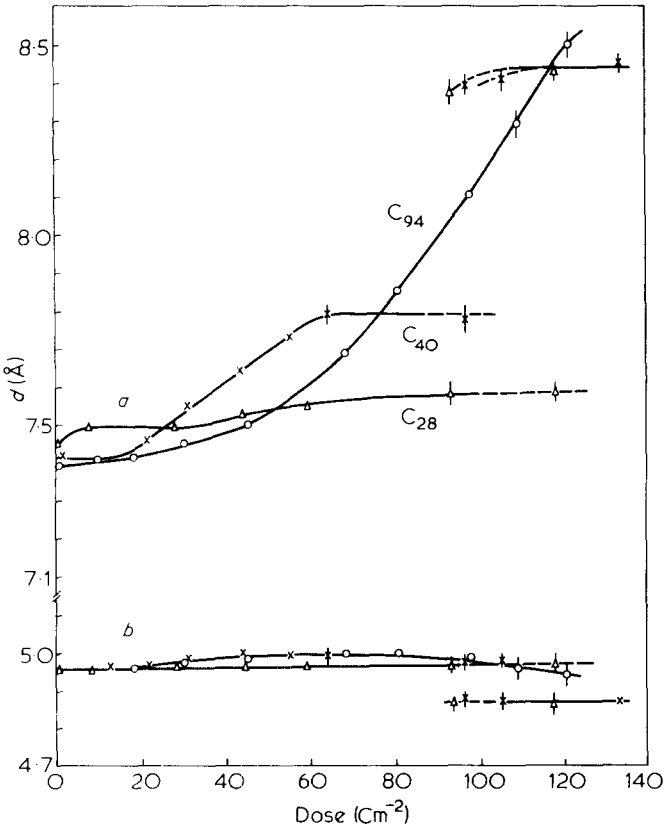

Figure 5 Dose dependence of crystal lattice parameters *a* and *b* for paraffins △, $C_{28}H_{58}$, x, $C_{40}H_{82}$; and ○, $C_{94}H_{190}$ irradiated at room temperature. Current density 100 mA m^{-2}. The new spacings below 4.9 Å and above 8.4 Å appearing at a dose just below 100 C m^{-2} are those of the hexagonal phase

Electron diffraction

In no case did lattice spacings remain constant during irradiation. For all paraffins, at all dose rates and temperatures, expansion of the orthorhombic unit cell was clearly detectable, primarily along the *a*-dimension. However, the extent to which the expansion occurred was highly dependent on all three variables investigated: chain length; temperature of irradiation; and dose rate. Some broadening of diffraction spots occurred in all cases, and was greater where changes in spacings were larger. Hexagonal lattice reflections appeared at high doses in most cases.

Figure 5 shows the change in lattice spacings for three paraffins of different chain length, $C_{28}H_{58}$, $C_{40}H_{82}$ and $C_{94}H_{190}$, irradiated at room temperature. In $C_{94}H_{190}$ and also in polyethylene (not shown) the lattice parameter, *a*, increases continuously following the familiar pattern of γ-irradiated PE (see *Figure* 5 in Part 1[1] and *Figure* 6 in Part 2[2]). However, in shorter paraffins the *a* spacing reaches a plateau. Diffraction spots remain rather sharp in $C_{28}H_{58}$, broaden moderately in $C_{40}H_{82}$ and greatly in $C_{94}H_{190}$ and in PE. Separate hexagonal $(100)_h$ reflections appear in $C_{28}H_{58}$ and $C_{40}H_{82}$ at doses below 100 C m^{-2}.

The effect of increasing the irradiation temperature is exemplified in *Figure* 6. Irradiation at higher temperatures produces less distortion of the lattice. Both the crystal spacings and the width of the diffraction spots are less affected.

The effect of changing the third variable, the dose rate, is illustrated in *Figure* 7 for room temperature irradiation of $C_{40}H_{82}$. A higher dose rate produces a larger lattice

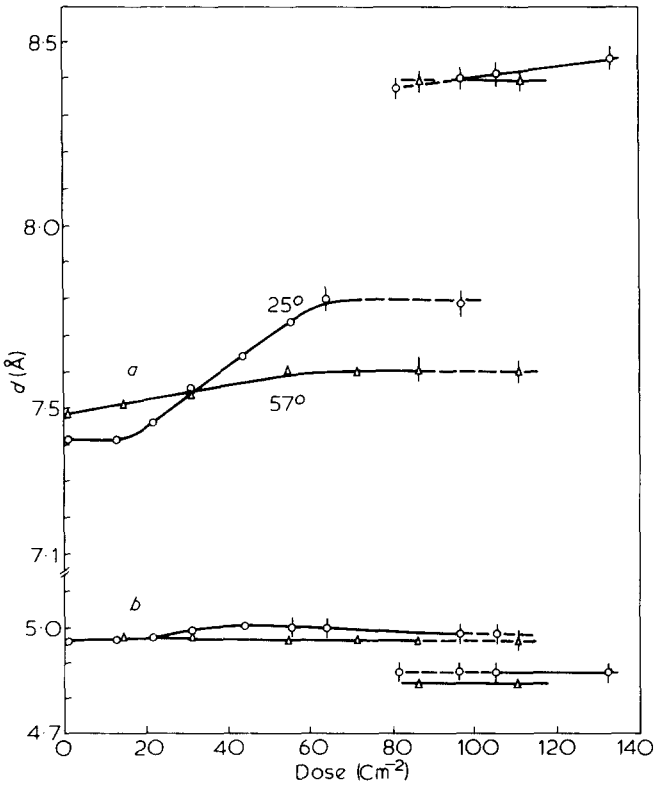

Figure 6 Dose dependence of the lattice parameters *a* and *b* for paraffin $C_{40}H_{82}$ at ○, 25°C and △, 57°C. Current density 100 mA m^{-2}

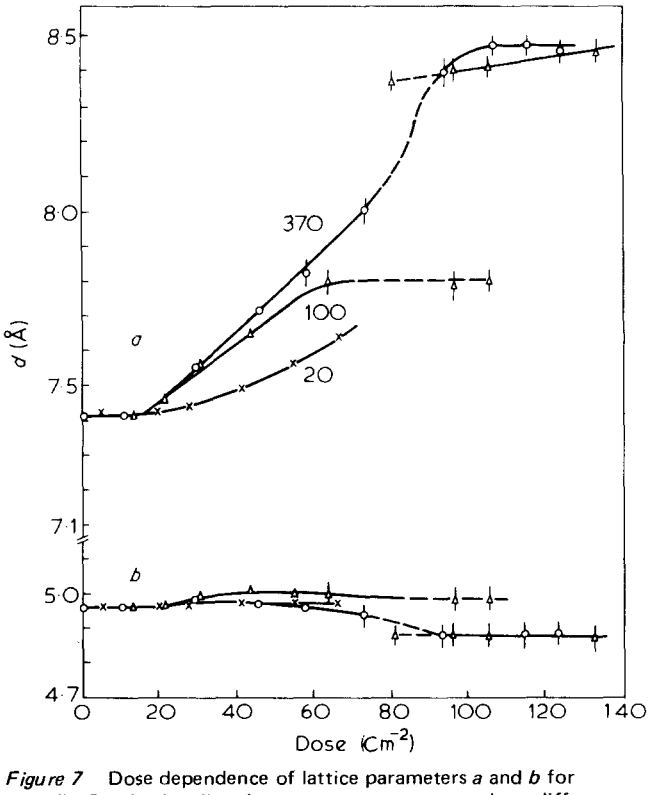

Figure 7 Dose dependence of lattice parameters *a* and *b* for paraffin $C_{40}H_{82}$ irradiated at room temperature at three different current densities: x, 20; △, 100; ○, 370 mA m^{-2}. At 20 mA m^{-2} irradiation was stopped before the diffraction spots disappeared completely

distortion for a given total dose than does a lower dose rate. The effect of changing the electron current on the temperature is much smaller than the deliberate changes of temperature, as in *Figure* 6, in the course of our experiments.)

The shortest paraffin studied, $C_{23}H_{48}$, behaved anomalously in the present experiments in many respects. This is because only a relatively small number of defects cause a phase transition from the normal orthorhombic (β_0) form to a new, highly mobile but still othorhombic modification (α_0) which is close in properties to the fully hexagonal 'rotator' phase (α_H)[12,13]. We carried out a series of experiments on $C_{23}H_{48}$ and the results will be reported in a separate paper. At present we shall only briefly describe one experiment in which a crystal was exposed to a beam of high intensity (0.4 A m^{-2}) for about 1 min at 25°C. This caused a phase transition and the *a* lattice spacing jumped from 7.46 to 7.70 Å. However, after the crystal was moved out of the beam and re-examined after 30 min the spacing was observed to have retracted back to 7.47 Å, i.e. the crystal transformed to the original undistorted β_0 modification.

DISCUSSION

The results of the electron microscope experiments substantiate the main conclusion derived from the calorimetric and X-ray investigation on γ-irradiated paraffins (Part 2[2]). Coexistence of a crystalline and a liquid phase in irradiated n-alkanes is directly observed here. This and additional observations have led to the recognition of three major new factors in the radiation response of crystalline paraffins, with potential implications for polyethylene (PE).

(1) From the existence and the characteristics of the non-diffracting patches, referred to here as droplets, it is concluded that there must exist a previously unsuspected, rapid transfer of radiation-induced active sites across the crystal.

(2) Substantial lattice distortion *can* be produced in paraffins, suggesting that there may be no basic distinction between PE and paraffins in this respect as might have appeared from Parts 1 and 2 alone.

(3) On the basis of at least one special case ($C_{23}H_{48}$ in the α_0 form) it is concluded that, once introduced, the lattice distortions due to crosslinks have the ability to heal out subsequently.

In what follows we shall discuss these three points in turn.

Droplets and their implications

The most salient observation is the existence of the droplets and their identification with the amorphous phase created by radiation. The previously observed[2] reduction in crystalline diffraction intensity and the corresponding increase in amorphous X-ray scattering with increasing radiation dose is thus identifiable with the formation and spreading of such droplets. At this point a note by Petermann and Gleiter[7] should be mentioned, which reports the formation of black patches in dark field images of crystals of a mixed paraffin. The above authors interpret those patches as distorted crystalline regions within a less distorted matrix. We consider that the black patches are equivalent to our droplets. From the quoted melting point we estimated that the paraffin used by them contained around 38 carbon atoms. The separation of the patches in their photographs was about 20 nm by our measurement. Such a high density of droplets is to be expected for paraffins of that chain length irradiated at room temperature. Our room temperature irradiation produced large droplets (average separation 1/4 μm) in $C_{28}H_{58}$, whereas in $C_{40}H_{82}$ the inhomogeneities, if formed at all, were already unresolvable under present experimental conditions. Thus, Petermann and Gleiter's results fit our scheme. However, the affected regions should by our evidence be amorphous (we see no evidence for a more and less distorted lattice in the diffraction patterns). In any event, the distinctness of the damaged regions implies clustering of the defects, with which we concur. Furthermore, the existence of heterogeneities on such a large scale as demonstrated in the present work calls for the postulation of an unexpectedly efficient transport of deposited energy through the crystals. As the energy deposition itself is necessarily homogenous, the present observation must mean that some intermediary (to be referred to as 'active species' or 'active site') is capable of migrating rapidly and thus to give rise to the observed inhomogeneities.

The next point to note is that the number of droplets in a given crystal region remains constant in the course of irradiation, the continuing effect of the damage being to increase their size. In the present situation this must mean that the radiation damage, and hence the underlying crosslinking itself, is produced only in certain localities. The extraordinarily high rate of droplet nucleation and growth rules out the alternative interpretation that the crosslinked molecules form at random and subsequently coalesce into droplets by solid state diffusion (segregation of crosslinks formed within the crystal lattice may possibly take place, but much more slowly — see below).

We enivisage the following sequence of events during irradiation of paraffins. First, the highly mobile active sites form uniformly throughout the crystal. As their concentration builds up they increasingly give rise to crosslinks. We know from electron diffraction that a small initial lattice distortion (increase in *a* lattice spacing, see *Figures* 5 and 6) occurs while the droplets are being formed. As this does not increase further it clearly corresponds to a slight damage spread uniformly across the crystal layer. Beyond a certain threshold concentration of defects liquid droplets would nucleate and act as sinks for newly forming mobile active sites. By previous experience relating to crosslinking[1] and to the decay rate of free radicals[14], termination of active species by crosslinking would occur in the liquid much more readily than in the crystalline phase. Consequently, once the initial droplet population is established, only a low steady state concentration of active sites would be maintained in the lattice, insufficient to cause much further crosslinking there. Thus nucleation of new droplets would cease. Instead, the existing droplets would become increasingly cross-linked and expand at the expense of the surrounding crystal, in full accord with observation. Moreoever, further molecules from the crystal will continuously dissolve in the droplets in order to maintain the equilibrium ratio of crosslinked and uncrosslinked paraffin in the liquid phase (see the phase diagram in Part 2[2]). Naturally, the liquid droplets will turn into a gel at some point.

The nucleation of a droplet itself could conceivably be merely the result of a chance fluctuation of the initial crosslink concentration. Nevertheless, there is reason to

think that once there is damage within the lattice this could induce further damage on continuing irradiation. Localized regions of higher lattice mobility are likely to from around crosslinks, by analogy with the increased mobility found in crosslinked PE lattice[15]. A higher mobility, in turn, facilitates crosslinking[1]. Due to their large radius of migration the active species can be selective and thus react mainly at such preferred sites of higher mobility. Hence, some clustering of crosslinks may be envisaged already at the earliest stage of irradiation facilitaing the nucleation of liquid droplets.

While the present evidence is insufficient for considering further details of droplet nucleation, we can nevertheless observe how this is affected by external variables within our control. The droplets are small and more numerous at lower irradiation temperature and at higher dose rates. This suggests that the diffusibility, and hence the range of migration, of the active species is lower at lower temperatures. This means a lower capture cross-section of the droplets, resulting in their larger number. The dose rate effect can be understood by attributing a certain finite lifetime to the active species. Accordingly, these will be more numerous at any given time for a high dose rate, thus giving rise again to a higher nucleation density of droplets.

So far we have been concerned with effects confined to a single crystal layer. As regards the multilayer nature of the crystals, we have seen that the droplets start to form first, and continue to expand fastest, in the overgrowth layer (as opposed to the first grown single layer of the crystal, see *Figure* 4). Furthermore, there is a distinct droplet-free belt in the single layer surrounding the overgrowth (see *Figures* 1 and 2). This is a puzzling effect as there is no clear reason for a higher concentration of primary active sites in the overgrowth. Since the geometry of the experiment was such that the overgrowth was at the exit side of the electron beam (*Figure* 4), the energy loss due to escape of secondary electrons must in fact have been larger in the overgrowth than in the single layer in contact with it[9]. It is rather more likely that the preference for droplet formation in the overgrowth comes from one of the following two reasons: (a) the initial concentration of crosslinks is more or less uniform through all the crystal layers, but the liquid phase nucleates more easily at the crystal–substrate interface; (b) crosslinks form preferentially at this interface. Which of the two is actually the case cannot be decided from the present evidence. Incidentally, the above effects do not seem to be due to some special property of carbon, since we ascertained that Formvar substrate acted in the same fashion.

In any event, once formed, the droplets in the overgrowth are supplied with active species produced both there and in the overlaying single layer. Hence they grow faster than their counterparts further away in the single layer. Moreover, the concentration of active sites in the single layer overlaying the overgrowth, as well as at a certain distance away from it, does not even reach the threshold necessary for nucleation of droplets: they are 'sucked in' into the overgrowth where the active species are consumed from a much earlier stage onwards in the course of the irradiation. This also accounts for the droplet-free zone surrounding the overgrowth in the single layer: the concentration of active sites cannot build up there sufficiently due to the above-mentioned influence of the overgrowth layer. As to be noted from the width of the droplet-free belt, the capture cross-section of the overgrowth has a range up to several microns. Such a large range is quite remarkable, particularly as it can only represent a lower limit for the migration range of the active species. Another important conclusion, already implied above, is the ability of the active sites to cross-over from one layer to the next.

The nature of the active species involved and the migration mechanism are not known. The current generally accepted view is that a crosslink in paraffins, as well as in PE, occurs by combination of two radiation-produced free radicals. Migration of the alkyl radical site has been postulated in PE crystals, where most of them diffuse to the fold surface to produce crosslinks[16,17]. The constant of the three-dimensional diffusion (D) for alkyl radical sites in PE has been estimated as 3×10^{-18} cm^2 s^{-1} [18] and 1×10^{-21} cm^2 s^{-1} [19] at room temperature. According to a crude estimate, D for the present migration of active sites in the paraffin crystals reaches at least 10^{-9} cm^2 s^{-1}.

Transfer of alkyl radical sites via the highly mobile 'hot' hydrogen atoms has been implied in the past[11]. However, simple calculation shows that most of the H-atoms would escape from the ultrathin crystals used here (10–20 nm) before having a chance to react further with another paraffin molecule. Thus 'hot' hydrogen cannot be identified with the present migratory active species.

A further point is that the phase separation which has been recognized in irradiated crystalline paraffins and, in particular, preferential crosslinking in one of the phases, inevitably implies that the statistics of random crosslinking cannot be applicable to such systems. Crosslinking statistics in γ-irradiated paraffins have been tested by one of us[20] using gel permeation chromatography (g.p.c.) for determining the molecular weight distribution. A more elaborate g.p.c. analysis, combined with the application of percolation statistics, has been performed by Dr Stejny in this laboratory. The latter work, being a major investigation in itself, requires separate reporting[21]. Invoking here only the main conclusion, both works have shown conclusively that once a molecule is crosslinked, its chance for further crosslinking is increased much more than can be expected from purely random introduction of crosslinks: i.e. for a given total fraction of crosslinked material, the amount of trimer and higher oligomers is higher, and the amount of dimer lower, than expected. Furthermore, gelation occurs at a dose where it would not yet be expected from the dimer/monomer ratio. The crosslinking reaction is thus truly non-random, as expected from a system where it occurs predominantly in a separate phase already rich in crosslinked molecules.

We thus see that, rather remarkably, the non-randomness of crosslinking is being brought out independently by three entirely different approaches: (1) by g.p.c. analysis combined with statistical considerations, only briefly referred to above, indicating non-randomness on the molecular level: (2) by thermal analysis leading to the concept of phase segregation (Part 2[2]); (3) by electron microscopy by which the segregated phase becomes directly visible, the main content of the present paper.

Lattice distortion

In Part 2[2] paraffins were presented as being distinct from PE as regards radiation damage. Their behaviour is characterized by a simultaneous reduction in the crystalline and an increase in the amorphous content on

irradiation with γ-rays. At the same time there is little or no damage in the remaining crystal lattice. We have seen that the model of phase separation provides an explanation for this behaviour (hereafter referred to as 'paraffin-like' or 'heterophase' behaviour). However, we have also seen that in the course of electron irradiation paraffins can reveal severe lattice damage. Hence the distinction between the 'heterophase' and the polyethylene-like 'homophase' behaviour is not as hard and fast as it first appeared. Under the present heading we shall summarize the circumstances under which such lattice damage occurs and discuss them in the light of the new knowledge.

It is immediately apparent that the occurrence of large distortion of the lattice is associated with the absence of liquid droplets and *vice versa*. Moreover, it will be clear that there is always an inverse relationship between the extent of lattice distortion and the nucleation density of droplets.

Effect of temperature. The overall experience, of which *Figure* 6 is an example, is that lowering of irradiation temperature increases lattice damage. Our irradiation experiments show that at low temperature (around -100°C) even the shorter paraffins behave similarly to PE at room temperature, i.e. large lattice distortion occurs. This is in line with the trend observed in connection with droplet formation, according to which, the range of migration of active species is reduced. This then leads to a higher concentration of active sites, more crosslinks in the lattice and hence more distortion before droplets appear. At suitably low temperatures no droplets form and extensive lattice damage results.

Effect of dose rate. Figure 7 gives an example of the general trend that a higher electron current leads to more pronounced lattice damage for a given total dose. As stated earlier this arises because a higher steady state concentration of active species produces a higher level of crosslinks within the lattice. Conversely, at lower dose rates the active species have more time to migrate to favourable locations. It is less likely that they will produce crosslinks within the lattice and more likely that they will find a droplet or an already existing crystal defect. We see that with a sufficiently low dose rate this would lead to behaviour characterizing the effect of γ-irradiation. Even at room temperature γ-irradiated paraffins as long as $C_{40}H_{82}$ would contain large amorphous regions and an undistorted crystal lattice. It will be recalled that the dose rate of our γ-irradiation was 2.7 Mrad h^{-1} (ref 2), which corresponds to an electron current density of approximately 0.3 mA m^{-2} under present experimental conditions[9].

Effect of chain length. Our experiments show that lattice damage caused by a given dose at a given temperature is higher if the paraffin is longer (*Figure* 5). We also find that paraffin $C_{94}H_{190}$ behaves at room temperature similarly to PE.

It will be apparent from the foregoing that a lower irradiation temperature, a higher dose rate and a greater chain length all lead to greater lattice damage. Likewise, in the case of the shorter paraffins, changing the above variables in the reverse direction leads to less lattice damage. Consequently, by varying these parameters in the appropriate direction, paraffins can be made to display PE-like behaviour (i.e. continuous lattice distortion with dose). Whether the opposite is also true, i.e. whether $C_{94}H_{190}$ and PE can be made to display paraffin-like 'heterophase' behaviour has not yet been clearly established. In $C_{94}H_{190}$ droplets could be observed when the irradiation temperature was sufficiently high. However, here we were only 9°C below the melting point so that more conventional premelting could not be fully discounted. 'Heterophase' behaviour in PE has not yet been observed, at least in experiments performed so far. Foremost of these is the electron diffraction work by Kiho and Ingram[5] who observed large changes in lattice parameters on electron irradiation carried out up to about 17°C below the melting point. Even if all the variables have not yet been explored it appears that with $C_{94}H_{190}$ and with PE, the newly discovered rapid migration of active sites, if present at all, occurs only at temperatures close to the melting point. By comparison, in $C_{40}H_{82}$ visible droplets form already more than 40°C below the melting temperature.

One brief point about the appearance of the hexagonal phase in irradiated paraffins (*Figures* 5–7): this is observed in almost all cases at high doses, shortly before the final disappearance of crystallinity. It may be that in addition to crosslinking, the hexagonal phase is favoured by other effects, such as accumulation of chain scission fragments or the severe reduction in size of the remaining crystalline phase.

Movement of defects formed

The healing out of damage with time has been observed so far only with crystals of $C_{23}H_{48}$ in the α_0 form, as described in the experimental section (crystals spontaneously transformed back into the undistorted β_0 form after irradiation ceased). Although the wider generality of the effect still needs to be established — in particular, whether it can also occur in the usual low-temperature orthorhombic lattice (β_0) — the mere fact that such an effect has been observed at all is of potential significance. Namely, it provides another route for phase segregation: instead of (or in addition to) the active sites migrating and producing crosslinks in the non-crystalline regions, we now have the possibility of the crosslinked molecules themselves segregating from the crystal lattice. Such segregation implies actual material transfer. This may well be restricted to crystal modifications with exceptionally high lattice mobility, such as the α_0 or the fully hexagonal α_H form[12]. Even so, the existence of the effect is significant and opens up a new window to radiation damage and to such further issues as compatibility and mobility of chains in crystalline paraffins. In the latter context we wish to draw attention to some recent findings along a different line, indicating quite unsuspected mobility of paraffin chains within the solid phase[22].

CONCLUSION TO THE SERIES

Crystallinity is destroyed by irradiation both in PE and in paraffins but *via* two different routes. In PE this occurs by increasing the number of defects (crosslinks) within the lattice which leads to large lattice distortion etc. ('homophase' process). In paraffins, at any given dose, an undistorted or only slightly disturbed crystalline phase coexists with a defect-containing liquid ('heterophase' process). These are two extreme cases observed in materials which were γ-irradiated at a low dose rate. High

dose rate electron irradiation of paraffins results in intermediate situations. Which way the paraffin will behave (with or without observable lattice distortion) depends on its chain length, irradiation temperature and the dose rate. However, the crystal lattice in PE is always damaged via the 'homophase' process, at least as far as observed to date.

The phase separation in irradiated paraffins is clearly the thermodynamically stable arrangement. In principle there may be two ways of achieving it: (i) the crosslinks themselves form in the liquid phase after such a phase has become nucleated at certain localities; (ii) the crosslinks are produced originally within the crystal lattice and become excluded from it subsequently. Electron microscope experiments showed that (i) does indeed occur, but this still may not be the whole story. Subsequent segregation of those crosslinks that may form within the lattice (case ii) has in fact been observed at least in the shortest paraffin ($C_{23}H_{48}$) examined by us so far.

Introduction of an increasing number of crosslinks into PE lattice at high irradiation doses was shown to cause the unusual thermal behaviour of such crystals with the orthorhombic→hexagonal transition occurring below the melting temperature (Part 1). The hexagonal modification is in itself interesting as it represents a state of order intermediate between the usual crystalline and amorphous polymeric phases. In addition, the evidence presented in Part 1 indicates its major role in bringing about the final destruction of crystallinity in PE subjected to high dose irradiation.

ACKNOWLEDGEMENT

We are indebted to Dr J. Stejny for numerous discussions including information on his own g.p.c. work bearing on the present subject. D. T. Grubb and G. Ungar wish to acknowledge financial support by the Science Research Council.

REFERENCES

1 Ungar, G. and Keller, A. *Polymer* 1980, **21**, 0000
2 Ungar, G. *Polymer* 1980, **21**, 000
3 Orth, H. and Fischer, E. W. *Makromol. Chem.* 1965, **88**, 188
4 Kobayashi, K. and Sakaoku, K. *Lab. Invest.* 1965, **14**, 359
5 Kiho, H. and Ingram, P. *Makromol. Chem.* 1968, **118**, 45
6 Siegal, G. *Z. Naturforsch.* (*A*) 1972, **27**, 325
7 Petermann, J. and Gleiter, H. *Kolloid Z. Z. Polym.* 1973, **251**, 850
8 Grubb, D. T. and Keller, A. 'Proc. 5th Congress Electron Microscopy', Manchester, Inst. Phys., London-Bristol 1972, p 554
9 Grubb, D. T. *J. Mater. Sci.* 1974, **9**, 1715
10 Grubb, D. T. *J. Phys.* (*E*) 1971, **4**, 222
11 Salovey, R. and Falconer, W. E. *J. Phys. Chem.* 1966, **70**, 3203
12 Müller, A. *Proc. Roy. Soc.* (*London*) 1932, **A138**, 514
13 Ungar, G., in preparation
14 Nara, S., Shimada, S., Kashiwabara, H. and Sohma, I. *J. Polym. Sci.* (*A*-2) 1968, **6**, 1435
15 Slichter, W. P. and Mandell, E. R. *J. Phys. Chem.* 1958, **62**, 334
16 Patel, G. N. and Keller, A. *J. Polym. Sci.* (*Polym. Phys. Edn*) 1975, **13**, 303
17 Patel, V. M. and Dole, M. *J. Polym. Sci.* (*Polym. Phys. Edn*) 1977, **15**, 907
18 Seguchi, T. and Tamura, R. *Rep. Prog. Polym. Phys. Jpn* 1971, **14**, 565
19 Shimada, S., Maeda, M. and Kashiwabara, H. *Polymer* 1977, **18**, 25
20 Ungar, G. *PhD Thesis*, University of Bristol (1979)
21 Stejny, J., in preparation
22 Ungar, G. and Keller, A. *Colloid Polym. Sci.* 1979, **257**, 90
23 Broadhurst, M. G. *J. Res. Nat. Bureau Stand.* (*A*) 1962, **66**, 241